Proceedings of the 28th IEEE
EMBS Annual International Conference
New York City, USA, Aug 30-Sept 3, 2006

Bio-Heat Transfer Model of Deep Brain Stimulation Induced Temperature changes

Maged M. Elwassif, Qingjun Kong, Maribel Vazquez, Marom Bikson*

Department of Biomedical Engineering, The City College of New York of The City University of New York

Abstract— **There is a growing interest in the use of chronic deep brain stimulation (DBS) for the treatment of medically refractory movement disorders and other neurological and psychiatric conditions. Fundamental questions remain about the physiologic effects and safety of DBS. Previous basic research studies have focused on the direct polarization of neuronal membranes by electrical stimulation. The goal of this paper is to provide information on the thermal effects of DBS using finite element models to investigate the magnitude and spatial distribution of DBS induced temperature changes. The parameters investigated include: stimulation waveform, lead selection, brain tissue electrical and thermal conductivity, blood perfusion, metabolic heat generation during the stimulation, Our results show that clinical Deep Brain Stimulation protocols will increase the temperature of surrounding tissue by up to 0.8ºC depending on stimulation/tissue parameters.**

I. Introduction

The electrical stimulation of tissue can lead to temperature increases as a result of both Joule heat and metabolic responses to stimulation [1]-[3],[5],[6]. Electrical stimulation-induced changes in temperature can profoundly affect tissue function; moderate temperature increases are not necessarily necrotic. The roles of temperature increases during clinical Deep Brain Stimulation (DBS) have not previously been considered.

Joule heat will be produced in any electrical field, where electrical currents are circulating [8]. The magnitude and spatial distribution of the induced temperature changes are a function of tissue properties and the electrical stimulation parameters.

Manuscript received April 21, 2006. This work was supported in part by Wallace H. Coulter foundation, P.S.C. CUNY Grant.

Maged M. Elwassif is with the Biomedical Engineering Department, The city college of New York of CUNY, New York, NY, 10031 (phone: 718 204 7930, email: melwassif@earthlink.net).

Qingjun Kong is with the Biomedical Engineering Department, The city college of New York of CUNY, New York, NY, 10031.(email: microseparation@yahoo.com

Maribel Vazquez is with the Biomedical Engineering Department, The city college of New York of CUNY, New York, NY, 10031. vazquez@ccny.cuny.edu

Marom Bikson is with the Biomedical Engineering Department, The city college of New York of CUNY, New York, NY, 10031(phone: 212 650 6791 email: bikson@ccny.cuny.edu).

Electrical stimulation has been used as a tool to analyze brain metabolism and related temperature rises [4]-[7]. Numerical models of radio-frequency ablation probes show that voltage greater than 10 V R.M.S. will increase temperature to 40°C or more [2],[3].

Brain function is especially sensitive to the changes in temperature. An increase in the temperature by ~ 1 °C can have profound effects on single neuron and neuronal network function [12]-[16]. Besides Joule heat, DBS may further increase brain temperature through increasing neuronal activity and concomitant metabolic activity, e.g. ion/neurotransmitter pumps [6],[17]. Indeed, DBS is generally associated with a local increase in metabolic activity [18],[19]. Both tissue heating and increased metabolic activity may promote increased blood flow as is observed during DBS [20].

Here we address, for the firs time, the potential scale of brain temperature increases resulting from clinical DBS protocols.

II. Model Method and Analysis

We developed a bio-heat transfer model for DBS using FEMLAB 3.2 (COMSOL Inc., Burlington, MA) adapting the Pennes homogenous blood perfusion model. During electrical stimulation (DBS), additional Joule heating arises when energy dissipated by an electric current flowing through a conductor is converted into thermal energy; modeled as $\sigma|\nabla V|^2$ where V is the local potential induced by stimulation. The resulting bioheat equation governs heating during electrical stimulation: [1], [3]

$$\rho C_p \frac{\partial T}{\partial t} = \nabla(k\nabla T) - \rho_b \omega_b C_b (T - T_b) + Q_m + \sigma|\nabla V|^2 \quad (1)$$

where k is the thermal conductivity of brain tissue (W/m·ºC) = 0.5-0.6, ρ is the density of brain tissue (kg/m^3) = 1040, C_p is the specific heat of brain tissue (J/kg·ºC) = 3650, σ is the electrical conductivity (S/m) = 0.15-0.35, ω_b is the volumetric blood perfusion rate per unit volume (ml/s/ml) = 0.004-0.012, ρ_b is the density of the blood (kg/m^3) =1057, C_b is the specific heat of blood (J/kg·ºC) =3600, T_b is the body core temperature = 37ºC

(in our stimulation) and Q_m is the metabolic heat source (we assumed Q_m =0 in this paper). All the above values are from references [9]-[11].

We considered two types of Medtronic leads (Fig. 1). We modeled a 'high' clinical DBS electrical setting (10 V, 185 pps and 210 μ sec) [21] using a constant V_{rms} of 1.56 Volt between the energized electrodes; Vrms was calculated from the root-mean-squared (r.m.s) voltage of the stimulation waveform. The DBS electrode shaft was modeled as electrically and thermally insulated, and we energized electrode 1 and 2 unless otherwise stated.

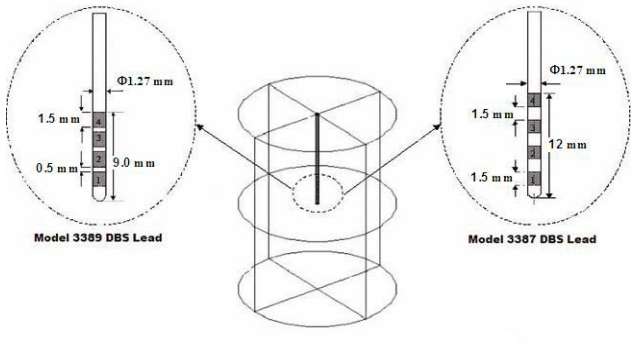

Fig.1: Schematic of model geometrical configuration. The DBS lead was positioned in the center of the tissue. Two DBS leads were modeled: the 3389 DBS lead with 1.5 mm electrodes and 0.5 mm spacing between electrodes (right); and the 3387 DBS lead with 1.5 mm electrodes and 1.5 spacing (left).

For the boundary conditions of the electrical field, the voltage between the two energized electrodes, either 1 and 4 (Fig. 2, *A* and *C*) or 1 and 2 (Fig. 2, *B* and *D*), was set to *Vrms*. The outer boundaries of the brain tissue were treaded as electrically insulated, namely $\partial V / \partial n = 0$. For the thermal boundary conditions, the temperature at the outer boundaries of the brain was fixed at 37°C and the DBS lead boundaries were thermally insolated. In this paper, we considered the steady state temperature increases consisted with continuous DBS and our interest to determine maximum temperature rises. The dimensions of the model were chosen to be large enough to abate boundary effects on the temperature and electrical field distribution. We modeled the Joule heat induced by DBS stimulation with the source term $\sigma|\nabla V|^2$. The local induced tissue electrical potential was determined by solving the Laplace equation $\nabla.(\sigma\nabla V) = 0$.

In this paper, we examined DBS induced temperature increases in two situations:

Case 1: Temperature distribution induced by DBS in a homogenous brain tissue without blood perfusion (ω_b=0).

Case 2: Temperature distribution induced by DBS in a homogenous brain tissue with blood perfusion.

III. RESULTS AND DISCUSSION

A. Temperature distribution induced by DBS in a homogenous brain tissue without blood perfusion

In our first iteration (Case 1), both ω_b and Q_m are zero. Initially, fixing electrical conductivity σ at 0.35 S/m and thermal conductivity k_t at 0.527 W/m·ºC , we found peak tissue temperature to range from 37.26 °C to 37.82 °C. As shown in figure 2 the temperature increase using Lead 3387 was roughly 0.2 °C lower than that using Lead 3389; this was because the Lead 3387 has a larger spacing distance between adjacent electrodes than Lead 3389. For similar reasons, for both lead types, the peak temperature increase is highly dependent on energized electrodes selection.

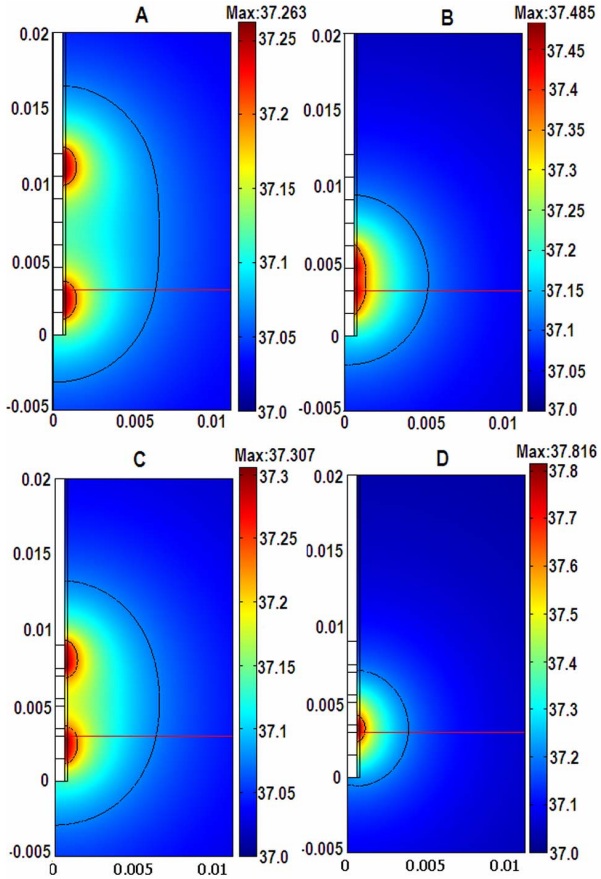

Fig. 2: Bio-heat transfer model of DBS. The false color maps indicate the spatial temperature distribution around the DBS electrodes, at σ =0.35 S/m, k_t=0.527 W/m·ºC, and ω=0. The red 'axial' line is the cross section at the proximal end of the most distal electrode; in the remaining figures the temperature profile is plotted along this line. 2A) Lead 3387, 1 and 4 electrodes were electrically energized. 2B) Lead 3387 1&2 electrodes were electrically energized. 2C) Lead 3389, 1 and 4 electrodes were electrically energized. 2D) Lead 3389 1and 2 electrodes were electrically energized.

We next investigated how tissue electrical conductivity and thermal conductivity affected the peak temperature and temperature spatial distribution in the brain tissue. We found that peak temperature rise (peak temperature -

baseline temperature) increased linearly with increasing electrical conductivity as shown in Fig. 3*A* and table 1-I, while peak temperature rise decreased linearly with the inverse of thermal conductivity increases as shown in Fig. 3*B* and table 1-II.

The temperature field space constant, defined here as the radial distance from the electrode that the temperature field decreased to 75% of is peak value (first contour line Fig. 2) (at the electrode surface) was not affected by changes in homogenous tissue electrical or thermal conductivity.

TABLE I
THE EFFECTS OF BIOLOGICAL PRAMETERS ON PEAK TEMPERATURE INDUCED BY DEEP BRAIN STIMULATION

	σ S/m	κ_t W/m·°C	ω_b ml/s/ml	T_{max} (°C)	
				3389 DBS lead	3387 DBS lead
I	0.15	0.527	0	37.35	37.21
	0.20			37.47	37.28
	0.30			37.70	37.42
	0.35			37.82	37.48
II	0.30	0.45	0	37.82	37.48
		0.50		37.74	37.44
		0.55		37.67	37.40
		0.60		37.62	37.37
III	0.30	0.527	0	37.70	37.42
			0.004	37.61	37.34
			0.008	37.57	37.31
			0.012	37.54	37.29

Where σ is the electrical conductivity , κ_t is the thermal conductivity, ϖ is the blood perfusion and T_{max} is the peak temperature

B. *Temperature distribution induced by DBS in a homogenous brain tissue with blood perfusion*

To study how the convection of blood regulates brain temperature during DBS, the blood perfusion rate, ω_b, was varied in our model from 0 to 0.012 ml/s/ml. In this paper blood temperature was fixed at 37°C. In this section (Case 2) the electrical conductivity and the thermal conductivity were fixed at 0.30 S/m and 0.527 W/m·ºC, respectively. The temperature increased to 37.42°C and 37.7°C with lead models 3387 and 3389 under these conditions without blood perfusion. The addition of blood perfusion convected Joule heat out of brain tissue so that the peak temperature decreased with increasing blood perfusion (Fig. 3C and table1-III). The peak temperature decreased moderately by 0.07°C and 0.12°C for Lead 3387 when the blood perfusion rates were 0.004 ml/s/ml and 0.012 ml/s/ml, respectively. Similarly, decreases by 0.09°C and 0.16°C occurred using Lead 3389 when the blood perfusion rates were 0.004 ml/s/ml and 0.012 ml/s/ml, respectively.

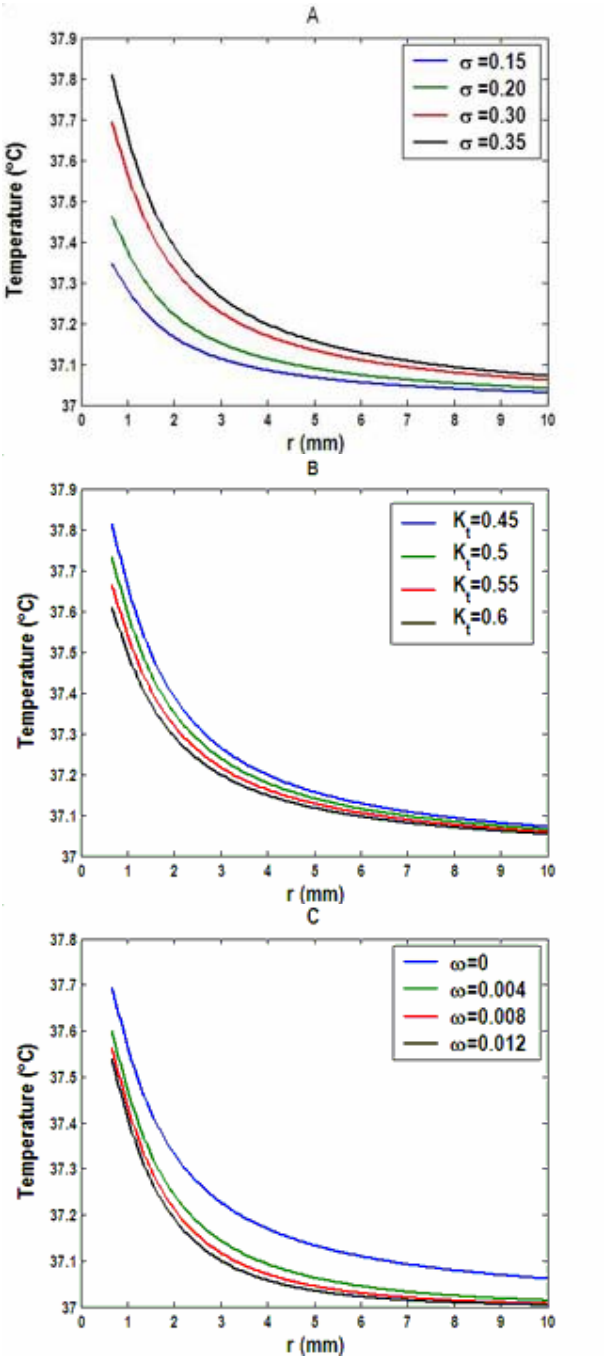

Fig. 3: Temperature distribution along the axial direction when the high setting (Lead 3389, electrodes 1 and 2 energized) was applied in a homogenous brain tissue. 3A) Temperature verses electrical conductivity (σ), the thermal conductivity (k_t) was fixed at 0.527 W/mºC and ω=0. Tissue temperature increased with increasing electrical conductivity. 3B) Temperature verses thermal conductivity,σ=0.3 S/m and ω=0. Tissue temperature decreased with increasing thermal conductivity (k_t). 3C) Temperature distribution verses blood perfusion; at (σ=0.30 S/m and k_t =0.527 W/mºC). Blood temperature was 37°C.

In contrast to the effects of changing tissue electrical/thermal conductivity, changes in blood perfusion rate effected brain temperature space constant; increasing perfusion rate decreased the space constant. Normally, the temperature of the blood going into the brain is a lower than that in brain tissue [9] and blood flow thus acts a heat sink.

IV. Conclusion

Our results predict that clinical DBS protocols can induce significant temperature rises in the surrounding brain tissue; the peak magnitude of these changes and their spatial distribution depend on a combination of stimulation waveform, electrode physical properties, and tissue properties. The precise magnitude and spatial distribution of temperature changes will determine the relevance of these changes to understanding the mechanisms of DBS. It is important to emphasize that DBS induced temperature rise is not proposed as a substitute for existing mechanisms of DBS action but as complimentary and critical for quantitative prediction of DBS effects. This study provides an initial basis for determining DBS safety ranges based on thermal considerations.

It is interesting to compare the spatial distribution of DBS induced thermal fields with 'neuronal activation fields' predicted by computer simulations [22] and the spatial extent of blood perfusion increases shown by imaging studies [23]. The simulated neuronal activation fields and the temperature fields considered here are only coincidentally of comparable orders. As noted above, we did not explicitly consider the effects of local neuronal activation on the temperature field. The temperature field may, in turn, affect the neuronal activation field through temperature-induced changed in neuronal firing threshold. Increases in imaged brain blood perfusion in response to DBS are also of comparable spatial order, suggesting they may represent a response to both increased neuronal activation and temperature increases.

Acknowledgment

We would like to thank Abhishek Datta and Thomas Radman for comments on an earlier version of this manuscript. This work was supported by the Whitaker Foundation and a PSC-CUNY award.

References

[1] Tungjitusolmun S., E. J. Woo, H. Cao. Finite element analyses of uniform current density electrodes for radio-frequency cardiac ablation. *IEEE Trans. Bio.Engr.,*2000; vol. 47, No.1:32-40.

[2] Labonte S. Numerical model for radio-frequency ablation of the endocardium and its experimental validation. *IEEE Trans. Bio.Eng*.1994; vol. 41, No. 2:108-115.

[3] Chang I. Finite Element Analysis of Hepatic Radiofrequency ablation probes using temperature-dependent electrical conductivity. *Biomedical Engineering Online* 2003, 2:12.

[4] LaManna JC, M Rosenthal, R Novack, DF Moffett, FF Jobsis. Temperature coefficients for the oxidative metabolic responses to electrical stimulation in cerebral cortex. *J Neurochem.*1980; 34(1): 203-9.

[5] LaManna JC, KA McCracken, M Patil, OJ Prohaska. Brain tissue temperature: activation-induced changes determined with a new multisensor probe. *Exp Med Biol.* 1988; 222: 383-9.

[6] LaManna JC, KA McCracken, M Patil, OJ Prohaska. Stimulus-activated changes in brain tissue temperature in the anesthetized rat. *Metab Brain Dis.* 1989; 4(4): 225-37.

[7] Tasaki I, PM Byrne. Heat production associated with synaptic transmission in the bullfrog spinal cord. *Brain Res.* 1987; 407(2): 386-9.

[8] Steffens H J, J Prescott. *Joule and concept of energy*: Science History Publications, New York 1979.

[9] Baysal U, J Haueisen. Use of a priori information in estimating tissue resistivities-application to human data in vivo. *Physiol. Meas*. 2004; 25: 737-748.

[10] Collins C, M Smith, R Turner. Model of local temperature changes in brain upon functional activation. *J. Appl. Physiol*., 2004; 97(6): 2051-2055.

[11] Xiaojiang X, P Tikuisis and G Giesbrecht. A mathematical model for human brain cooling during cold-water near-drowning. *Journal of Applied Physiology* 86:265-272, 1999.

[12] Hoffmann HM, VE Dionne. Temperature dependence of ion permeation at the endplate channel. J Gen Physiol. 1983; 81(5): 687-703

[13] Moser E, I Mathiesen, P Andersen. Association between brain temperature and dentate field potentials in exploring and swimming rats. *Science*.1993; 259(5099):1324-6

[14] Stiles JR, IV Kovyazina, EE Salpeter, Salpeter MM. The temperature sensitivity of miniature endplate currents is mostly governed by channel gating: evidence from optimized recordings and Monte Carlo simulations. Biophys J.1999; 77(2): 1177-87.

[15] Bennetts B, ML Roberts, AH Bretag, GY Rychkov. Temperature dependence of human muscle ClC-1 chloride channel. J Physiol. 2001; 535(Pt 1): 83-93

[16] Fujii S, H Sasaki, K Ito, K Kaneko, H Kato. Temperature dependence of synaptic responses in guinea pig hippocampal CA1 neurons in vitro. Cell Mol Neurobiol. 2002; 22(4): 379-91.

[17] Abbott BC, JV Howarth, JM Ritchie. The initial heat production associated with the nerve impulse in crustacean and mammalian non-myelinated nerve fibres. *J Physiol.* 1965; 178: 368-83.

[18] Zonenshayn, M., A.Y. Mogilner and A.R. Rezai. Neurostimulation and functional brain imaging. *Neurol Res* 2000; 22: 318–325

[19] McIntyre CC, M Savasta, L Kerkerian, L Goff, JL Vitek. Uncovering the mechanism(s) of action of deep brain stimulation: activation, inhibition, or both. *Clin Neurophysiol*.2004b; 115(6): 1239-48.

[20] J.S. Perlmutter; J.W. Mink; A.J. Bastian; K. Zackowski; T. Hershy; E. Miyawaki; W. Koller and T.O. Videen, Blood flow responses to Deep Brain Stimulation of thalamus. *Neurology* 2002; 58: 1388-1394.

[21] Implant Manual. Medtonic 3387,3389 lead kit for Deep Brain Stimulation (2003).

[22] Christophor R. B, C McIntyre. Tissue and electrode capacitance reduce neural activation volumes during deep brain stimulation. *Clinical Neurophysiology* 116 (2005) 2490- 2500.

[23] J.S. Perlmutter; J.W. Mink; A.J. Bastian; K. Zackowski; T. Hershy; E. Miyawaki; W. Koller and T.O. Videen, Blood flow responses to Deep Brain Stimulation of thalamus. *Neurology* 2002; 58: 1388-1394.